Electronic Supplementary Material (ESI) for Physical Chemistry Chemical Physics.

Supporting Information: Bare *versus* Protected Tetrairidium Clusters by Density Functional Theory

Maurício J. Piotrowski,[*,†] Glaucio R. Nagurniak,[†] Eder H. da Silva,[‡] and Renato L. T. Parreira[‡]

†*Department of Physics, Federal University of Pelotas, PO Box* 354, 96010 – 900, *Pelotas, RS, Brazil*

‡*Núcleo de Pesquisas em Ciências Exatas e Tecnológicas, Universidade de Franca, Franca, SP Brazil*

E-mail: mauriciomjp@gmail.com

Phone: +55 53 3275 7542

A Convergence tests

Here, we show some methodological tests to determine the main parameters used in our calculations, which are described in the Computational Details section. In Tables 1, 2, 3, and 4 we have showed some properties for the specific case of a protected square Ir_4 cluster (i.e., square Ir_4 with four PH_3 molecules) and for the non-protected (bare) square Ir_4 cluster, as a function of the parameters: cubic box side (*box*), cutoff energy (*encut*), and the break conditions for the electronic self-consistent-loop (*EDiff*) and for the ionic relaxation loop (*EDiffg*). To exemplify, we show the test results for the properties: the energetic difference between the total energies of Ir_4 with and without PH_3 molecules (ΔE_{tot}), the average bond lengths for the nanoclusters (d_{av}), the effective coordination numbers for the nanoclusters (ECN), and the total magnetic moments (m_T) for the systems Ir_4 (structure *A*) and Ir_4+4 PH_3 (structure *pA*).

Table 1: Convergence tests for the box size: the relative total energies ($\Delta E_{\mathbf{tot}} = E_{\mathbf{tot}}^{\mathbf{pA}} - E_{\mathbf{tot}}^{\mathbf{A}}$), the average bond lengths for the nanoclusters ($d_{av}^{\mathbf{A}}$ and $d_{av}^{\mathbf{pA}}$), the effective coordination numbers for the nanoclusters ($\mathbf{ECN^A}$ and $\mathbf{ECN^{pA}}$), and the total magnetic moments ($m_{\mathbf{T}}^{\mathbf{A}}$ and $m_{\mathbf{T}}^{\mathbf{pA}}$) for $\mathbf{Ir_4}$ and $\mathbf{Ir_4}$+4 $\mathbf{PH_3}$. These calculations were performed using a 480 eV **cutoff energy and convergence criteria of** 1.0×10^{-6} eV **(energy) and** 0.015 eV/Å **(force).**

box (Å)	ΔE_{tot} (eV)	d_{av}^{A} (Å)	d_{av}^{pA} (Å)	$\mathrm{ECN^A}$	$\mathrm{ECN^{pA}}$	$m_{\mathrm{T}}^{\mathrm{A}}$ (μ_{B})	$m_{\mathrm{T}}^{\mathrm{pA}}$ (μ_{B})
12	−69.58	2.34	2.38	2.00	2.00	8.00	2.00
14	−69.57	2.34	2.38	2.00	2.00	8.00	2.00
16	−69.57	2.34	2.38	2.00	2.00	8.00	2.00
18	−69.57	2.34	2.38	2.00	2.00	8.00	2.00
20	−69.57	2.34	2.38	2.00	2.00	8.00	2.00
22	−69.57	2.34	2.38	2.00	2.00	8.00	2.00

Table 2: Convergence tests for the cutoff energy: the relative total energies ($\Delta E_{\mathbf{tot}} = E_{\mathbf{tot}}^{\mathbf{pA}} - E_{\mathbf{tot}}^{\mathbf{A}}$), the average bond lengths for the nanoclusters ($d_{av}^{\mathbf{A}}$ and $d_{av}^{\mathbf{pA}}$), the effective coordination numbers for the nanoclusters ($\mathbf{ECN^A}$ and $\mathbf{ECN^{pA}}$), and the total magnetic moments ($m_{\mathbf{T}}^{\mathbf{A}}$ and $m_{\mathbf{T}}^{\mathbf{pA}}$) for $\mathbf{Ir_4}$ and $\mathbf{Ir_4}$+4 $\mathbf{PH_3}$. These calculations were performed using a cubic box with side of 20 Å **and convergence criteria of** 1.0×10^{-6} eV **(energy) and** 0.015 eV/Å **(force). The ENMAX value is equal to** 319.843 eV**.**

encut (eV)	ΔE_{tot} (eV)	d_{av}^{A} (Å)	d_{av}^{pA} (Å)	$\mathrm{ECN^A}$	$\mathrm{ECN^{pA}}$	$m_{\mathrm{T}}^{\mathrm{A}}$ (μ_{B})	$m_{\mathrm{T}}^{\mathrm{pA}}$ (μ_{B})
0.75xENMAX	−69.09	2.31	2.36	2.00	2.00	8.00	2.00
0.85xENMAX	−69.30	2.34	2.38	2.00	2.00	8.00	2.00
1.00xENMAX	−69.43	2.34	2.38	2.00	2.00	8.00	2.00
1.15xENMAX	−69.57	2.34	2.38	2.00	2.00	8.00	2.00
1.25xENMAX	−69.57	2.34	2.38	2.00	2.00	8.00	2.00
1.50xENMAX	−69.57	2.34	2.38	2.00	2.00	8.00	2.00
1.75xENMAX	−69.58	2.34	2.38	2.00	2.00	8.00	2.00
2.00xENMAX	−69.58	2.34	2.36	2.00	2.00	8.00	2.00
2.15xENMAX	−69.58	2.34	2.38	2.00	2.00	8.00	2.00

Table 3: Convergence test for the energy criterion (electronic convergence): the relative total energies ($\Delta E_{\mathbf{tot}} = E_{\mathbf{tot}}^{\mathbf{pA}} - E_{\mathbf{tot}}^{\mathbf{A}}$), the average bond lengths for the nanoclusters ($d_{av}^{\mathbf{A}}$ and $d_{av}^{\mathbf{pA}}$), the effective coordination numbers for the nanoclusters ($\mathbf{ECN^A}$ and $\mathbf{ECN^{pA}}$), and the total magnetic moments ($m_{\mathbf{T}}^{\mathbf{A}}$ and $m_{\mathbf{T}}^{\mathbf{pA}}$) for $\mathbf{Ir_4}$ and $\mathbf{Ir_4}$+4 $\mathbf{PH_3}$. These calculations were performed using a cubic box with side of 20 Å**,** 480 eV **cutoff energy, and convergence criterion of** 0.015 eV/Å **(force).**

EDiff (eV)	ΔE_{tot} (eV)	d_{av}^{A} (Å)	d_{av}^{pA} (Å)	$\mathrm{ECN^A}$	$\mathrm{ECN^{pA}}$	$m_{\mathrm{T}}^{\mathrm{A}}$ (μ_{B})	$m_{\mathrm{T}}^{\mathrm{pA}}$ (μ_{B})
10^{-3}	−69.57	2.34	2.38	2.00	2.00	8.00	2.00
10^{-4}	−69.57	2.34	2.38	2.00	2.00	8.00	2.00
10^{-5}	−69.57	2.34	2.38	2.00	2.00	8.00	2.00
10^{-6}	−69.57	2.34	2.38	2.00	2.00	8.00	2.00
10^{-7}	−69.57	2.34	2.38	2.00	2.00	8.00	2.00

Table 4: Convergence test for the force criterion (ionic convergence): the relative total energies ($\Delta E_{\mathbf{tot}} = E^{\mathbf{pA}}_{\mathbf{tot}} - E^{\mathbf{A}}_{\mathbf{tot}}$), the average bond lengths for the nanoclusters ($d^{\mathbf{A}}_{av}$ and $d^{\mathbf{pA}}_{av}$), the effective coordination numbers for the nanoclusters ($\mathbf{ECN^{A}}$ and $\mathbf{ECN^{pA}}$), and the total magnetic moments ($m^{\mathbf{A}}_{\mathbf{T}}$ and $m^{\mathbf{pA}}_{\mathbf{T}}$) for $\mathbf{Ir_4}$ and $\mathbf{Ir_4}$+4 $\mathbf{PH_3}$. These calculations were performed using a cubic box with side of 20 Å**,** 480 eV **cutoff energy, and convergence criterion of** 1.0×10^{-6} eV **(energy).**

EDiffg (eV/Å)	ΔE_{tot} (eV)	d^{A}_{av} (Å)	d^{pA}_{av} (Å)	$\mathrm{ECN^{A}}$	$\mathrm{ECN^{pA}}$	$m^{\mathrm{A}}_{\mathrm{T}}$ (μ_{B})	$m^{\mathrm{pA}}_{\mathrm{T}}$ (μ_{B})
0.005	−69.56	2.34	2.38	2.00	2.00	8.00	2.00
0.010	−69.57	2.34	2.38	2.00	2.00	8.00	2.00
0.015	−69.57	2.34	2.38	2.00	2.00	8.00	2.00
0.025	−69.57	2.34	2.38	2.00	2.00	8.00	2.00
0.050	−69.57	2.34	2.38	2.00	2.00	8.00	2.00

B Ir_4 Isomers

In Table 5 are presented the main properties for Ir_4 isomers, for which, we have included the main structural configurations. The results are obtained using DFT-PBE, DFT-PBE+vdW, DFT-PBE+SOC, and DFT-PBE+vdW+SOC calculations. The properties include the relative total energy for every atomic configuration (j) with respect to the square structure (a), i.e., $\Delta E_{\mathrm{tot}} = E^{(j)}_{\mathrm{tot}} - E^{(\mathrm{a})}_{\mathrm{tot}}$; the binding energy per atom, $E_b = E^{(j)}_{tot} - E^{\text{free-atom}}_{tot}$; the effective coordination number, ECN; the average weighted bond length, d_{av}; and the total magnetic moment, m_{T}.

C Square and Tetrahedral Magnetic Isomers

In Table 6 are presented the main properties for square and tetrahedral Ir_4 magnetic isomers, the results are obtained using the plain DFT-PBE calculations. The properties include the relative total energy for every magnetic isomer in relation to the respective lowest energy configuration, ΔE_{tot}; the binding energy per atom, E_b; the effective coordination number, ECN; the average weighted bond length, d_{av}; and the total magnetic moment, m_{T}.

Table 5: The relative total energy between Ir_4 isomers and square configuration (a) (ΔE_{tot}), the binding energy per atom (E_b), the total magnetic moment (m_T) (shown in parenthesis), the effective coordination number (ECN), and the average bond length (d_{av}) for Ir_4 structures from plain DFT-PBE, DFT-PBE+vdW, DFT-PBE+SOC, and DFT-PBE+vdW+SOC calculations.

Ir_4	ΔE_{tot} [eV]				E_b (m_T) [eV/atom (μ_B)]			
(j)	PBE	PBE+vdW	PBE+SOC	PBE+vdW+SOC	PBE	PBE+vdW	PBE+SOC	PBE+vdW+SOC
(a) square	0.00	0.00	0.00	0.00	−3.64 (8.0)	−3.66 (8.0)	−3.61 (3.7)	−3.67 (3.7)
(b) butterfly	0.84	0.86	0.91	0.91	−3.43 (4.0)	−3.45 (4.0)	−3.38 (2.6)	−3.44 (2.6)
(c) rhombus	0.93	1.03	0.96	0.96	−3.41 (8.0)	−3.40 (6.0)	−3.37 (5.1)	−3.43 (5.1)
(d) triangle-cap	1.22	1.20	1.07	1.04	−3.34 (4.0)	−3.36 (4.0)	−3.34 (2.2)	−3.41 (2.2)
(e) tetrahedron	1.42	1.47	1.45	1.50	−3.29 (0.0)	−3.29 (0.0)	−3.24 (0.0)	−3.29 (0.0)
(f) zigzag	2.08	1.72	1.59	1.52	−3.12 (4.0)	−3.23 (4.0)	−3.21 (1.8)	−3.28 (1.2)
(g) line	2.58	2.56	2.79	2.76	−3.00 (0.0)	−3.02 (0.0)	−2.91 (1.4)	−2.98 (1.4)
Ir_4	ECN				d_{av} [Å]			
(j)	PBE	PBE+vdW	PBE+SOC	PBE+vdW+SOC	PBE	PBE+vdW	PBE+SOC	PBE+vdW+SOC
(a) square	2.00	2.00	1.99	1.99	2.34	2.34	2.31	2.31
(b) butterfly	2.38	2.38	2.39	2.40	2.38	2.38	2.38	2.39
(c) rhombus	2.47	2.49	2.49	2.48	2.44	2.42	2.44	2.44
(d) triangle-cap	1.97	1.97	1.97	1.97	2.32	2.32	2.33	2.32
(e) tetrahedron	3.00	3.00	2.99	2.99	2.45	2.45	2.46	2.46
(f) zigzag	1.50	1.50	1.50	1.50	2.24	2.24	2.25	2.25
(g) line	1.50	1.50	1.50	1.50	2.22	2.22	2.22	2.22

Table 6: The relative total energy between Ir_4 magnetic isomers and the lowest energy configuration for the square and tetrahedral clusters (ΔE_{tot}), the binding energy per atom (E_b), the effective coordination number (ECN), the average bond length (d_{av}), and the total magnetic moment (m_T) for Ir_4 magnetic structures from plain DFT-PBE calculations.

Isomers	m_T (μ_B)	ΔE_{tot} (eV)	E_b (eV/atom)	ECN	d_{av} (Å)
square	0.0	0.29	−3.57	2.00	2.31
	2.0	0.29	−3.57	1.98	2.30
	4.0	0.12	−3.61	1.99	2.31
	6.0	0.15	−3.60	2.00	2.32
	7.0	0.14	−3.61	2.00	2.33
	8.0	0.00	−3.64	2.00	2.34
	9.0	0.52	−3.51	2.00	2.36
	10.0	0.96	−3.40	1.99	2.39
tetrahedral	0.0	0.00	−3.29	3.00	2.45
	1.0	0.19	−3.24	3.00	2.45
	2.0	0.25	−3.23	2.99	2.46
	4.0	0.43	−3.18	2.96	2.48
	8.0	0.70	−3.12	2.99	2.51

D CO, O_2, PH_3, and SH_2 Molecules

In Table 7 are presented the main properties for gas-phase molecules used as ligands, i.e., CO, O_2, PH_3, and SH_2 molecules, the results are obtained using the DFT-PBE, DFT-PBE+vdW, DFT-

PBE+SOC, and DFT-PBE+vdW+SOC calculations. The properties include the binding energy per atom, E_b; the average bond length, d_0 (C−O, O−O, P−H, and S−H); and the total magnetic moment, m_{T}.

Table 7: The binding energy per atom (E_b), the average bond length (d_0), and the total magnetic moment (m_{T}) for CO, O_2, PH_3, and SH_2 molecules, using DFT-PBE, DFT-PBE+vdW, DFT-PBE+SOC, and DFT-PBE+vdW+SOC calculations.

DFT	E_b^{CO} (eV/atom)	d_{av}^{CO} (Å)	$m_{\mathrm{T}}^{\mathrm{CO}}$ (μ_{B})	$E_b^{\mathrm{O_2}}$ (eV/atom)	$d_{av}^{\mathrm{O_2}}$ (Å)	$m_{\mathrm{T}}^{\mathrm{O_2}}$ (μ_{B})	$E_b^{\mathrm{PH_3}}$ (eV/atom)	$d_{av}^{\mathrm{PH_3}}$ (Å)	$m_{\mathrm{T}}^{\mathrm{PH_3}}$ (μ_{B})	$E_b^{\mathrm{SH_2}}$ (eV/atom)	$d_{av}^{\mathrm{SH_2}}$ (Å)	$m_{\mathrm{T}}^{\mathrm{SH_2}}$ (μ_{B})
PBE	−5.75	1.14	0.0	−3.04	1.23	2.0	−2.60	1.43	0.0	−2.63	1.35	0.0
PBE+vdW	−5.75	1.14	0.0	−3.04	1.23	2.0	−2.60	1.43	0.0	−2.63	1.35	0.0
PBE+SOC	−5.75	1.14	0.0	−3.04	1.23	2.0	−2.60	1.43	0.0	−2.64	1.35	0.0
PBE+vdW+SOC	−5.75	1.14	0.0	−3.04	1.23	2.0	−2.60	1.43	0.0	−2.64	1.35	0.0

E Ligands Adsorption on Ir_4

In Table 8 are shown the main properties for $Ir_4(Mol)_n$ systems, where Mol is equal to CO, O_2, PH_3, and SH_2, and $n = 0, 1, 4$, and $n = 12$ just for CO case, including (i) the relative total energy, ΔE_{tot}, between systems with tetrahedral and square isomers; (ii) the adsorption energy, $E_{ad} = (E_{tot}^{\mathrm{Ir_4}(Mol)_n} - E_{tot}^{\mathrm{Ir_4}} - nE_{tot}^{Mol})/n$, where n is the number of ligands and $E_{tot}^{\mathrm{Ir_4}(Mol)_n}$, $E_{tot}^{\mathrm{Ir_4}}$, and E_{tot}^{Mol} are the total energies of the adsorbed systems, Ir_4 cluster, and the ligands, respectively; (iii) ECN for Ir_4; (iv) d_{av} for Ir_4; and (v) m_{T} for $Ir_4(Mol)_n$ systems, obtained by DFT-PBE, DFT-PBE+vdW, DFT-PBE+SOC, and DFT-PBE+vdW+SOC calculations.

Table 8: The relative total energy between systems with tetrahedral and square Ir_4 isomers (ΔE_{tot}), the adsorption energy (E_{ad}), the total magnetic moment (m_T) for $Ir_4(Mol)_n$ systems (shown in parenthesis), the effective coordination number (ECN) for Ir_4, and the average bond length (d_{av}) for Ir_4, considering DFT-PBE, DFT-PBE+vdW, DFT-PBE+SOC, and DFT-PBE+vdW+SOC calculations.

Systems	ΔE_{tot} [eV]				E_{ad} (m_T) [eV/ligand (μ_B)]			
	PBE	PBE+vdW	PBE+SOC	PBE+vdW+SOC	PBE	PBE+vdW	PBE+SOC	PBE+vdW+SOC
Ir_4^{sq}	0.00	0.00	0.00	0.00	– (8.0)	– (8.0)	– (3.7)	– (3.7)
Ir_4^{te}	1.42	1.47	1.45	1.50	– (0.0)	– (0.0)	– (0.0)	– (0.0)
$Ir_4(CO)^{sq}$	0.00	0.00	0.00	0.00	−2.32 (2.0)	−2.52 (4.0)	−2.45 (3.8)	−2.50 (3.7)
$Ir_4(CO)^{te}$	0.64	0.84	0.83	0.88	−3.10 (2.0)	−3.16 (2.0)	−3.07 (1.1)	−3.12 (1.0)
$Ir_4(O_2)^{sq}$	0.00	0.00	0.00	0.00	−2.25 (4.0)	−2.23 (2.0)	−2.28 (2.5)	−2.33 (2.3)
$Ir_4(O_2)^{te}$	0.61	0.60	0.72	0.77	−3.06 (2.0)	−3.10 (2.0)	−3.01 (1.5)	−3.05 (1.5)
$Ir_4(PH_3)^{sq}$	0.00	0.00	0.00	0.00	−1.92 (4.0)	−1.72 (0.0)	−1.85 (2.9)	−1.94 (3.1)
$Ir_4(PH_3)^{te}$	1.61	1.35	1.65	1.69	−1.74 (0.0)	−1.84 (0.0)	−1.65 (0.0)	−1.75 (0.0)
$Ir_4(SH_2)^{sq}$	0.00	0.00	0.00	0.00	−1.51 (4.0)	−1.58 (4.0)	−1.32 (1.8)	−1.40 (1.8)
$Ir_4(SH_2)^{te}$	1.37	1.40	1.25	1.29	−1.57 (2.0)	−1.65 (2.0)	−1.53 (1.5)	−1.61 (1.5)
$Ir_4(CO)_4^{sq}$	0.00	0.00	0.00	0.00	−2.34 (2.0)	−2.39 (2.0)	−2.30 (0.0)	−2.35 (0.0)
$Ir_4(CO)_4^{te}$	−1.38	−1.40	−1.37	−1.39	−3.04 (0.0)	−3.11 (0.0)	−3.01 (0.0)	−3.07 (0.0)
$Ir_4(O_2)_4^{sq}$	0.00	0.00	0.00	0.00	−2.28 (0.0)	−2.32 (0.0)	−2.24 (0.9)	−2.28 (0.5)
$Ir_4(O_2)_4^{te}$	−0.39	−0.35	−0.40	−0.40	−2.73 (0.0)	−2.77 (0.0)	−2.70 (0.0)	−2.75 (0.0)
$Ir_4(PH_3)_4^{sq}$	0.00	0.00	0.00	0.00	−1.80 (0.0)	−1.89 (0.0)	−1.77 (0.0)	−1.86 (0.0)
$Ir_4(PH_3)_4^{te}$	−0.25	−0.32	−0.22	−0.29	−2.22 (0.0)	−2.34 (0.0)	−2.19 (0.0)	−2.31 (0.0)
$Ir_4(SH_2)_4^{sq}$	0.00	0.00	0.00	0.00	−1.42 (0.0)	−1.50 (0.0)	−1.38 (0.0)	−1.46 (0.0)
$Ir_4(SH_2)_4^{te}$	0.75	0.72	0.74	0.71	−1.59 (0.0)	−1.68 (0.0)	−1.56 (0.0)	−1.65 (0.0)
$Ir_4(CO)_{12}^{sq}$	0.00	0.00	0.00	0.00	−1.98 (0.0)	−2.06 (0.0)	−1.95 (0.0)	−2.03 (0.0)
$Ir_4(CO)_{12}^{te}$	−1.65	−1.78	−1.64	−1.76	−2.23 (0.0)	−2.33 (0.0)	−2.21 (0.0)	−2.31 (0.0)
Systems	ECN				d_{av} [Å]			
	PBE	PBE+vdW	PBE+SOC	PBE+vdW+SOC	PBE	PBE+vdW	PBE+SOC	PBE+vdW+SOC
Ir_4^{sq}	2.00	2.00	1.99	1.99	2.34	2.34	2.31	2.31
Ir_4^{te}	3.00	3.00	2.99	2.99	2.45	2.45	2.46	2.46
$Ir_4(CO)^{sq}$	2.00	2.00	1.99	1.99	2.32	2.32	2.33	2.33
$Ir_4(CO)^{te}$	2.86	2.86	2.88	2.88	2.47	2.47	2.48	2.48
$Ir_4(O_2)^{sq}$	1.99	2.00	2.00	2.00	2.33	2.32	2.33	2.33
$Ir_4(O_2)^{te}$	2.91	2.91	2.92	2.92	2.45	2.45	2.46	2.46
$Ir_4(PH_3)^{sq}$	2.00	2.00	2.00	2.00	2.32	2.32	2.32	2.32
$Ir_4(PH_3)^{te}$	2.74	2.74	2.79	2.79	2.48	2.48	2.49	2.49
$Ir_4(SH_2)^{sq}$	2.00	2.00	2.00	2.00	2.32	2.32	2.32	2.32
$Ir_4(SH_2)^{te}$	2.74	2.75	2.77	2.77	2.45	2.45	2.46	2.46
$Ir_4(CO)_4^{sq}$	2.00	2.00	2.00	2.00	2.38	2.38	2.38	2.38
$Ir_4(CO)_4^{te}$	2.98	2.99	2.99	2.99	2.54	2.54	2.54	2.54
$Ir_4(O_2)_4^{sq}$	2.00	2.00	2.00	2.00	2.32	2.32	2.32	2.32
$Ir_4(O_2)_4^{te}$	2.39	2.38	2.38	2.39	2.40	2.40	2.40	2.40
$Ir_4(PH_3)_4^{sq}$	2.00	2.00	2.00	2.00	2.36	2.36	2.37	2.37
$Ir_4(PH_3)_4^{te}$	2.98	2.98	2.98	2.98	2.53	2.53	2.53	2.53
$Ir_4(SH_2)_4^{sq}$	2.00	2.00	2.00	2.00	2.34	2.34	2.35	2.35
$Ir_4(SH_2)_4^{te}$	2.99	2.99	2.99	2.99	2.50	2.50	2.51	2.51
$Ir_4(CO)_{12}^{sq}$	2.41	2.41	2.41	2.41	2.81	2.81	2.82	2.81
$Ir_4(CO)_{12}^{te}$	3.00	3.00	3.00	3.00	2.74	2.74	2.74	2.74

F CO, O_2, PH_3, and SH_2 Adsorption on Ir_4

In Table 9 are shown the main properties for only one CO, O_2, PH_3, and SH_2 molecule adsorbed on Ir_4 clusters, for some energetic isomers. For these calculations, all nonequivalent sites were considered, including the three nonequivalent adsorption sites (top, bridge, and hollow). The properties include the relative total energy, ΔE_{tot}, between the different adsorption site structures and the lowest energy configuration; the adsorption energy, E_{ad}; ECN for Ir_4; d_{av} for Ir_4; and m_{T} for $Ir_4(Mol)$ systems, obtained by DFT-PBE, DFT-PBE+vdW, DFT-PBE+SOC, and DFT-PBE+vdW+SOC calculations.

Table 9: The relative total energies among the adsorption sites, where the lowest energy configuration is the referential ($\Delta E_{\mathbf{tot}}$), the adsorption energy (E_{ad}), the effective coordination number (ECN) for $\mathbf{Ir_4}$, the average bond length (d_{av}) for $\mathbf{Ir_4}$, and the total magnetic moment ($m_{\mathbf{T}}$) for $\mathbf{Ir_4}(Mol)$ systems, considering DFT-PBE, DFT-PBE+vdW, DFT-PBE+SOC, and DFT-PBE+vdW+SOC calculations. The most stable isomers are square (sq), tetrahedron (te), and butterfly (bu).

Systems	Site	ΔE_{tot} [eV]				E_{ad} (m_{T}) [eV (μ_{B})]			
		PBE	PBE+vdW	PBE+SOC	PBE+vdW+SOC	PBE	PBE+vdW	PBE+SOC	PBE+vdW+SOC
$Ir_4(CO)^{sq}$	top	0.00	0.01	0.00	0.12	−2.48 (4.0)	−2.52 (4.0)	−2.45 (3.1)	−2.39 (1.7)
$Ir_4(CO)^{sq}$	top	0.16	0.00	0.01	0.00	−2.32 (2.0)	−2.52 (4.0)	−2.45 (3.8)	−2.50 (3.7)
$Ir_4(CO)^{sq}$	bridge	0.50	0.48	0.59	0.57	−1.98 (6.0)	−2.04 (6.0)	−1.86 (3.9)	−1.93 (3.9)
$Ir_4(CO)^{te}$	top	0.80	0.84	0.84	0.88	−3.10 (2.0)	−3.16 (2.0)	−3.07 (1.1)	−3.12 (1.0)
$Ir_4(CO)^{te}$	bridge	1.02	1.07	1.11	1.15	−2.88 (0.0)	−2.93 (0.0)	−2.79 (0.0)	−2.84 (0.0)
$Ir_4(CO)^{bu}$	hollow	1.46	0.99	1.50	1.50	−1.87 (6.0)	−2.39 (2.0)	−1.86 (3.9)	−1.91 (3.6)
$Ir_4(CO)^{te}$	hollow	1.52	1.57	1.56	1.60	−2.38 (2.0)	−2.43 (2.0)	−2.35 (1.3)	−2.39 (1.3)
$Ir_4(O_2)^{sq}$	top	0.00	0.00	0.00	0.00	−2.25 (4.0)	−2.23 (2.0)	−2.28 (2.5)	−2.33 (2.3)
$Ir_4(O_2)^{bu}$	top	0.28	0.24	0.40	0.42	−2.82 (2.0)	−2.86 (2.0)	−2.79 (1.5)	−2.82 (1.5)
$Ir_4(O_2)^{sq}$	top	0.29	0.24	0.29	0.30	−1.96 (4.0)	−1.99 (4.0)	−1.99 (1.1)	−2.03 (1.0)
$Ir_4(O_2)^{te}$	top	0.61	0.60	0.72	0.77	−3.06 (2.0)	−3.10 (2.0)	−3.01 (1.5)	−3.05 (1.5)
$Ir_4(O_2)^{te}$	top	1.22	0.80	1.33	1.38	−2.46 (2.0)	−2.90 (2.0)	−2.40 (0.2)	−2.44 (0.2)
$Ir_4(O_2)^{sq}$	bridge	1.67	1.65	0.36	1.71	−0.58 (4.0)	−0.58 (2.0)	−1.91 (1.9)	−0.62 (1.9)
$Ir_4(O_2)^{te}$	bridge	2.74	2.71	2.87	2.90	−0.93 (2.0)	−1.00 (2.0)	−0.86 (1.3)	−0.93 (1.3)
$Ir_4(PH_3)^{sq}$	top	0.00	0.07	0.00	0.00	−1.92 (4.0)	−1.72 (0.0)	−1.85 (2.9)	−1.94 (3.1)
$Ir_4(PH_3)^{sq}$	top	0.22	0.00	0.03	0.03	−1.71 (0.0)	−1.79 (0.0)	−1.82 (2.7)	−1.91 (2.6)
$Ir_4(PH_3)^{bu}$	top	1.20	1.00	1.08	1.27	−1.57 (4.0)	−1.65 (4.0)	−1.68 (1.9)	−1.59 (1.7)
$Ir_4(PH_3)^{te}$	bridge	1.61	1.42	1.65	1.69	−1.74 (0.0)	−1.84 (0.0)	−1.65 (0.0)	−1.75 (0.0)
$Ir_4(PH_3)^{bu}$	hollow	1.68	1.57	1.68	1.67	−1.09 (6.0)	−1.08 (4.0)	−1.08 (3.8)	−1.19 (3.9)
$Ir_4(PH_3)^{te}$	bridge	2.17	1.99	1.96	2.00	−1.18 (6.0)	−1.27 (6.0)	−1.34 (2.7)	−1.44 (2.6)
$Ir_4(PH_3)^{sq}$	hollow	2.19	1.98	1.98	1.98	0.27 (2.0)	0.19 (2.0)	0.12 (3.2)	0.04 (3.2)
$Ir_4(SH_2)^{sq}$	top	0.00	0.00	0.00	0.00	−1.51 (4.0)	−1.58 (4.0)	−1.32 (1.8)	−1.40 (1.8)
$Ir_4(SH_2)^{sq}$	top	0.33	0.32	0.14	0.14	−1.18 (6.0)	−1.26 (6.0)	−1.19 (3.7)	−1.25 (3.5)
$Ir_4(SH_2)^{sq}$	top	0.37	0.36	0.27	0.26	−1.14 (6.0)	−1.22 (6.0)	−1.05 (1.8)	−1.14 (0.8)
$Ir_4(SH_2)^{te}$	top	1.37	1.40	1.25	1.29	−1.57 (2.0)	−1.65 (2.0)	−1.53 (1.5)	−1.61 (1.5)
$Ir_4(SH_2)^{te}$	bridge	2.11	2.13	1.74	1.77	−0.83 (6.0)	−0.92 (6.0)	−1.04 (1.6)	−1.12 (1.2)
$Ir_4(SH_2)^{te}$	bridge	2.46	2.49	2.36	2.39	−0.48 (2.0)	−0.57 (2.0)	−0.42 (1.4)	−0.50 (1.4)
$Ir_4(SH_2)^{bu}$	bridge	2.63	2.64	2.52	2.53	0.27 (4.0)	0.20 (4.0)	0.29 (2.6)	0.22 (2.7)
Systems	Site	ECN				d_{av} [Å]			
		PBE	PBE+vdW	PBE+SOC	PBE+vdW+SOC	PBE	PBE+vdW	PBE+SOC	PBE+vdW+SOC
$Ir_4(CO)^{sq}$	top	2.00	2.00	1.99	2.00	2.32	2.32	2.33	2.33
$Ir_4(CO)^{sq}$	top	2.00	2.00	1.99	1.99	2.32	2.32	2.33	2.33
$Ir_4(CO)^{sq}$	bridge	1.99	1.99	1.99	1.99	2.37	2.38	2.37	2.38
$Ir_4(CO)^{te}$	top	2.86	2.86	2.88	2.88	2.47	2.47	2.48	2.48
$Ir_4(CO)^{te}$	bridge	2.79	2.79	2.81	2.81	2.49	2.49	2.49	2.49
$Ir_4(CO)^{bu}$	hollow	2.47	2.43	2.47	2.47	2.48	2.44	2.48	2.48
$Ir_4(CO)^{te}$	hollow	2.89	2.89	2.90	2.90	2.50	2.50	2.51	2.51
$Ir_4(O_2)^{sq}$	top	1.99	2.00	2.00	2.00	2.33	2.32	2.33	2.33
$Ir_4(O_2)^{bu}$	top	2.49	2.49	2.49	2.49	2.39	2.39	2.39	2.40
$Ir_4(O_2)^{sq}$	top	2.00	2.00	2.00	2.00	2.33	2.33	2.32	2.32
$Ir_4(O_2)^{te}$	top	2.91	2.91	2.92	2.92	2.45	2.45	2.46	2.46
$Ir_4(O_2)^{te}$	top	2.59	2.49	2.60	2.59	2.43	2.40	2.43	2.43
$Ir_4(O_2)^{sq}$	bridge	1.97	2.00	2.00	1.98	2.33	2.33	2.32	2.33
$Ir_4(O_2)^{te}$	bridge	2.68	2.68	2.66	2.66	2.45	2.45	2.45	2.45
$Ir_4(PH_3)^{sq}$	top	2.00	2.00	2.00	2.00	2.32	2.32	2.32	2.32
$Ir_4(PH_3)^{sq}$	top	2.00	2.00	2.00	2.00	2.32	2.32	2.32	2.32
$Ir_4(PH_3)^{bu}$	top	2.49	2.49	2.48	2.49	2.42	2.42	2.42	2.42
$Ir_4(PH_3)^{te}$	bridge	2.74	2.74	2.79	2.79	2.48	2.48	2.49	2.49
$Ir_4(PH_3)^{bu}$	hollow	2.46	2.43	2.46	2.45	2.48	2.46	2.47	2.47
$Ir_4(PH_3)^{te}$	bridge	2.77	2.76	2.84	2.83	2.53	2.53	2.51	2.51
$Ir_4(PH_3)^{sq}$	hollow	1.99	1.99	2.00	2.00	2.37	2.37	2.37	2.38
$Ir_4(SH_2)^{sq}$	top	2.00	2.00	2.00	2.00	2.32	2.32	2.32	2.32
$Ir_4(SH_2)^{sq}$	top	2.00	2.00	2.00	2.00	2.34	2.34	2.32	2.32
$Ir_4(SH_2)^{sq}$	top	2.00	2.00	2.00	2.00	2.34	2.34	2.34	2.34
$Ir_4(SH_2)^{te}$	top	2.74	2.75	2.77	2.77	2.45	2.45	2.46	2.46
$Ir_4(SH_2)^{te}$	bridge	2.89	2.89	2.98	2.98	2.54	2.54	2.50	2.50
$Ir_4(SH_2)^{te}$	bridge	2.64	2.63	2.64	2.64	2.44	2.44	2.45	2.45
$Ir_4(SH_2)^{bu}$	bridge	2.40	2.40	2.40	2.41	2.43	2.43	2.44	2.44

G Contours of Deformation Densities

Bellow, we provided the contours of deformation densities, $\Delta\rho_1$, $\Delta\rho_2$, and $\Delta\rho_3$, for the cases of $Ir_4(CO)_4^{sq}$, $Ir_4(CO)_4^{te}$, $Ir_4(CO)_{12}^{sq}$, and $Ir_4(CO)_{12}^{te}$ in Figure 1, and for the cases of $Ir_4(PH_3)_4^{sq}$, $Ir_4(PH_3)_4^{te}$, $Ir_4(SH_2)_4^{sq}$, $Ir_4(SH_2)_4^{te}$, $Ir_4(O_2)_4^{sq}$, and $Ir_4(O_2)_4^{te}$ in Figure 2.

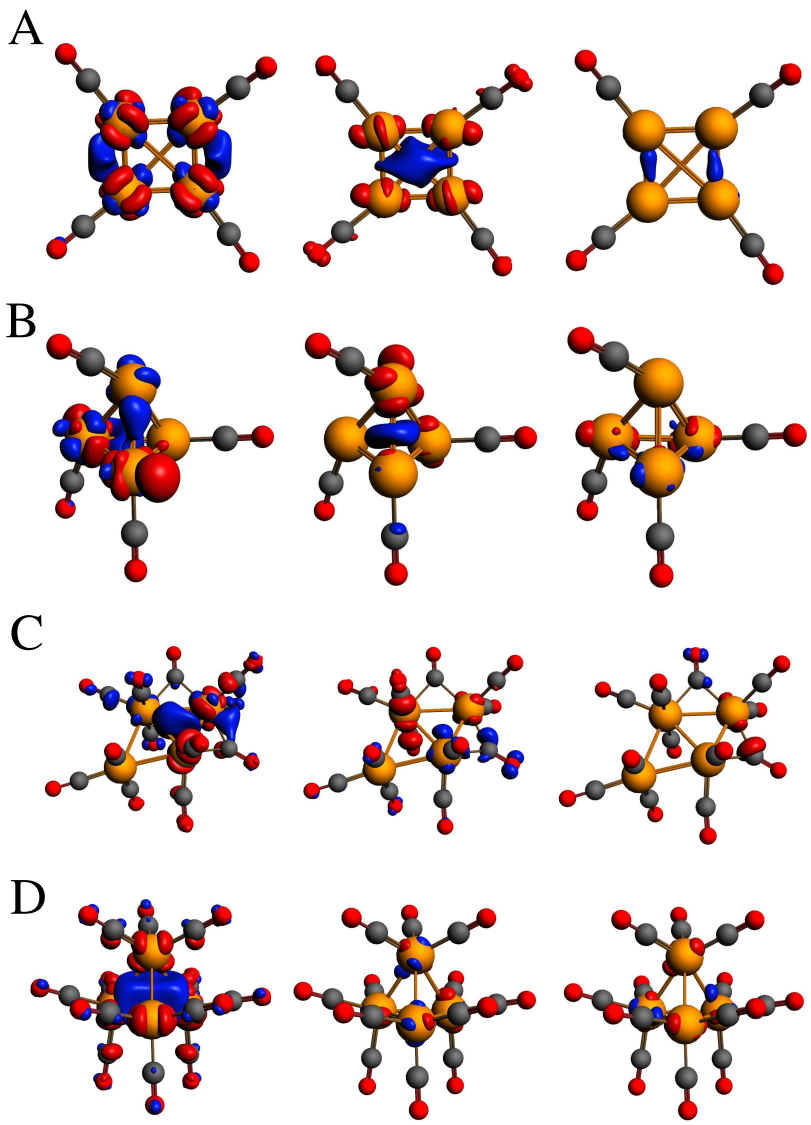

Figure 1: Contours of deformation densities, $\Delta\rho_1$, $\Delta\rho_2$, and $\Delta\rho_3$ of $Ir_4(CO)_4^{sq}$ (A), $Ir_4(CO)_4^{te}$ (B), $Ir_4(CO)_{12}^{sq}$ (C), and $Ir_4(CO)_{12}^{te}$ (D). The flux of charge densities are given from red (decrease in charge density) to blue (increase in charge density) surface orbitals. The cutoff value was set as 0.0065 a.u. for all cases.

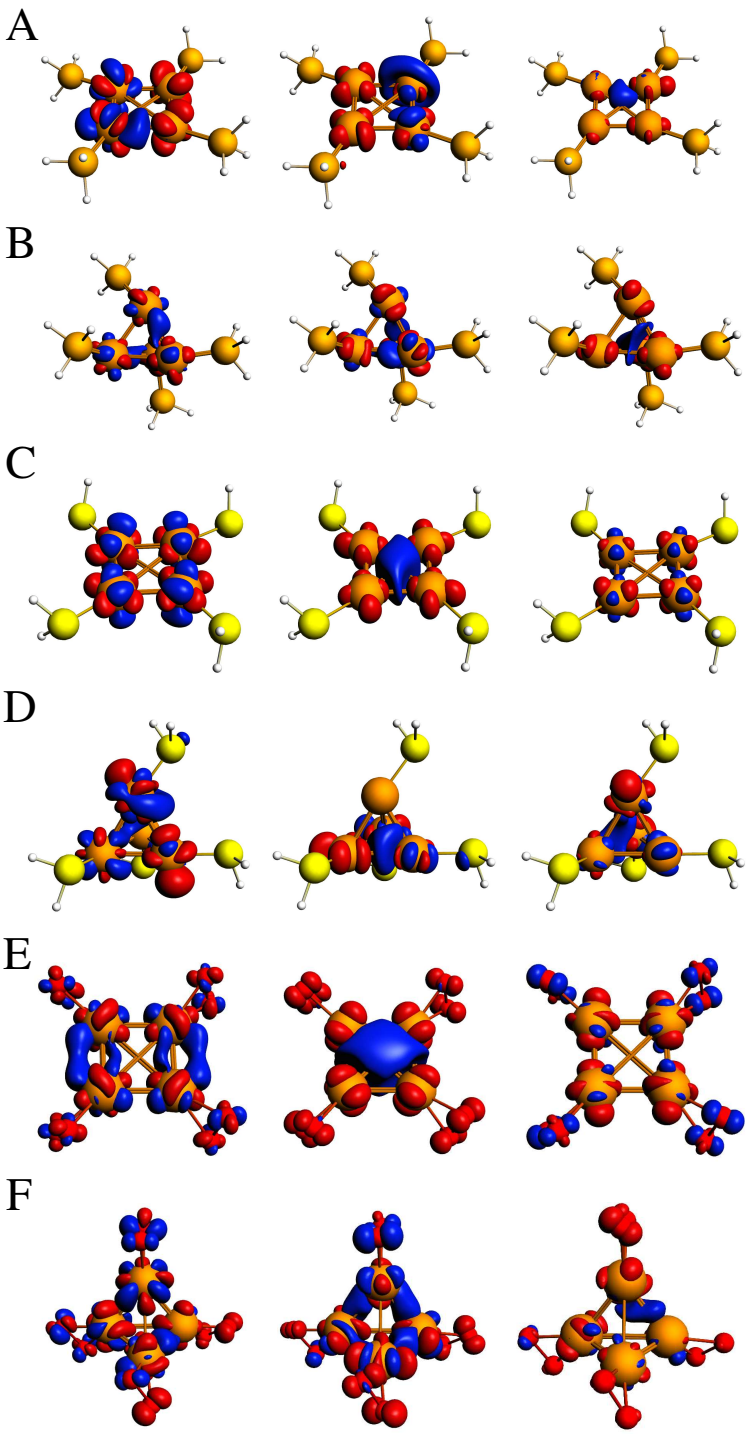

Figure 2: Contours of deformation densities, $\Delta\rho_1$, $\Delta\rho_2$, and $\Delta\rho_3$ of $Ir_4(PH_3)_4{}^{sq}$ (A), $Ir_4(PH_3)_4{}^{te}$ (B), $Ir_4(SH_2)_4{}^{sq}$ (C), $Ir_4(SH_2)_4{}^{te}$ (D), $Ir_4(O_2)_4{}^{sq}$ (E), and $Ir_4(O_2)_4{}^{te}$ (F). The flux of charge densities are given from red (decrease in charge density) to blue (increase in charge density) surface orbitals. The cutoff value was set as 0.0065 a.u. for all cases.

Bellow, we provided the contours of deformation densities, $\Delta\rho_1$, $\Delta\rho_2$, and $\Delta\rho_3$, for the cases of $Ir_4(CO)^{te}$, $Ir_4(CO)_4{}^{te}$, $Ir_4(O_2)^{te}$, and $Ir_4(O_2)_4{}^{te}$ in Figure 3, and for the cases of $Ir_4(PH_3)^{te}$, $Ir_4(PH_3)_4{}^{te}$, $Ir_4(SH_2)^{te}$, and $Ir_4(SH_2)_4{}^{te}$ in Figure 4.

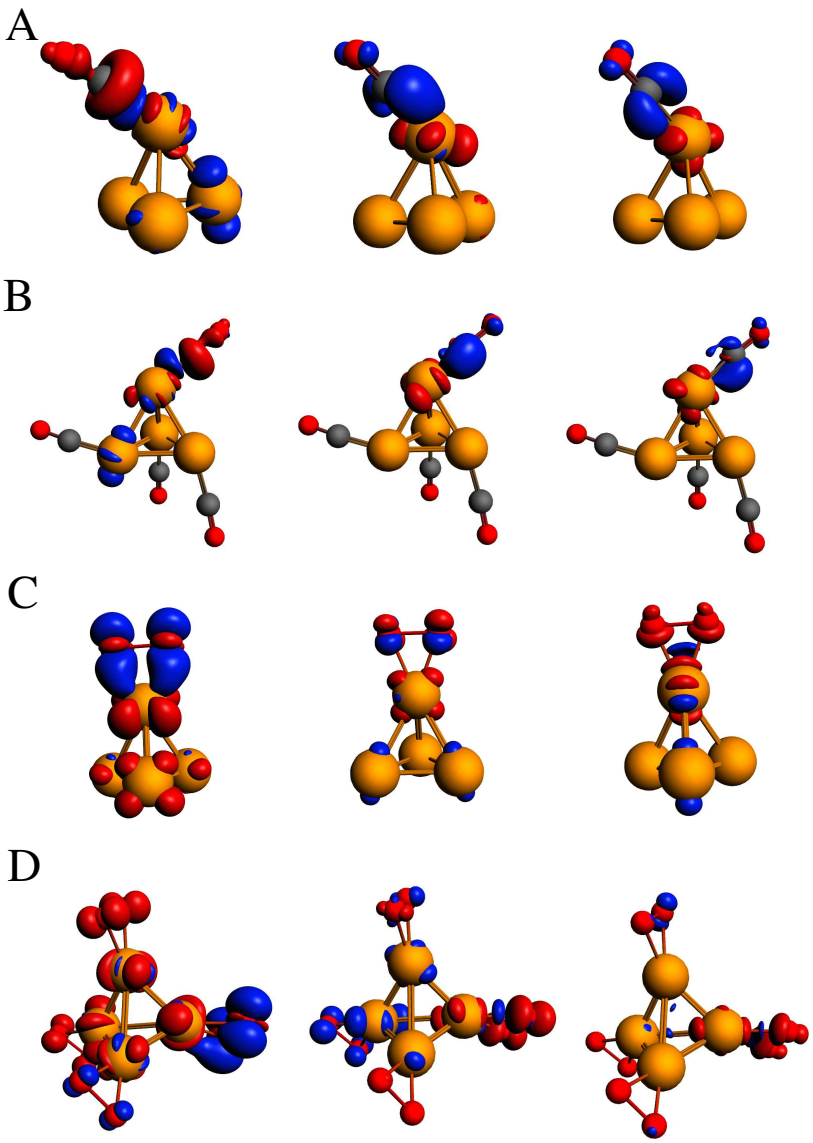

Figure 3: Contours of deformation densities, $\Delta\rho_1$, $\Delta\rho_2$, and $\Delta\rho_3$ of $Ir_4(CO)^{te}$ (A), $Ir_4(CO)_4{}^{te}$ (B), $Ir_4(O_2)^{te}$ (C), and $Ir_4(O_2)_4{}^{te}$ (D). The flux of charge densities are given from red (decrease in charge density) to blue (increase in charge density) surface orbitals. The cutoff value was set as 0.0065 a.u. for all cases.

H Energy Decomposition Analysis

To improve the understanding about the ligand$\cdots$$Ir_4$ interactions, we carried out DFT-PBE+vdW+SOC geometries and splitted each one, in two fragments, lingand and tetrahedral Ir_4 motif, in order to analyze the fragments interaction by EDA-NOCV approach. The results are shown in Table 10.

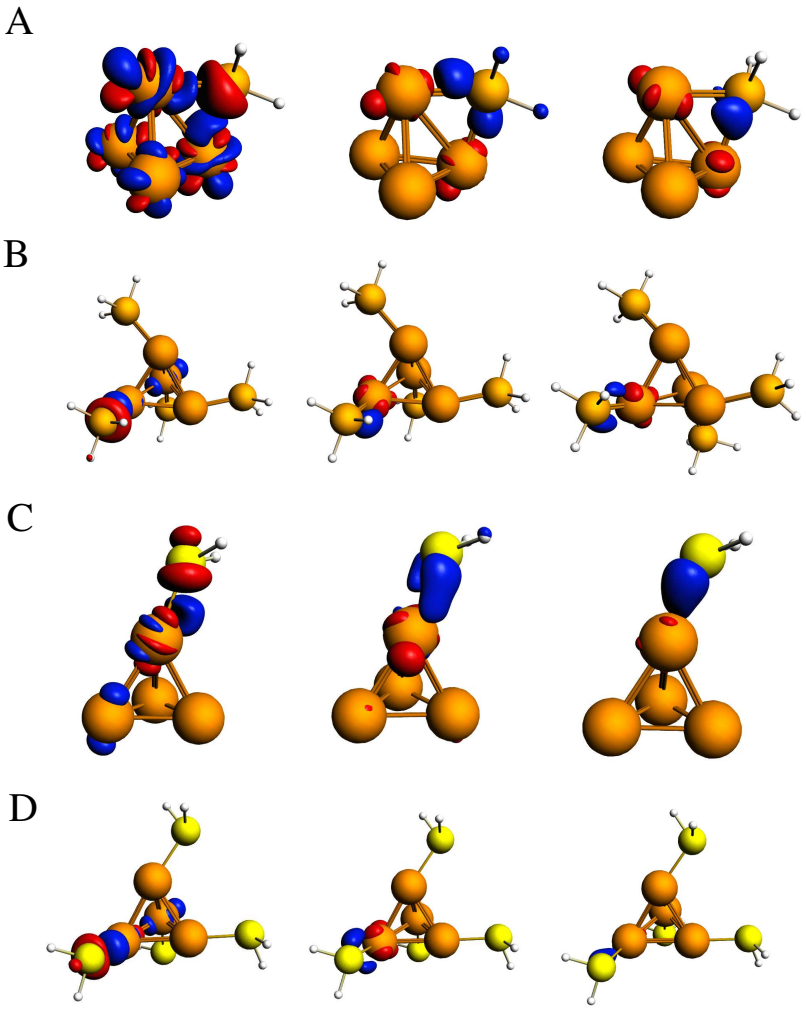

Figure 4: Contours of deformation densities, $\Delta\rho_1$, $\Delta\rho_2$, and $\Delta\rho_3$ of $Ir_4(PH_3)^{te}$ (A), $Ir_4(PH_3)_4{}^{te}$ (B), $Ir_4(SH_2)^{te}$ (C), and $Ir_4(SH_2)_4{}^{te}$ (D). The flux of charge densities are given from red (decrease in charge density) to blue (increase in charge density) surface orbitals. The cutoff value was set as 0.0065 a.u. for all cases.

Table 10: The EDA-NOCV analysis of ligand$\cdots$$Ir_4$ (ligand is equal to CO, O_2, PH_3, and SH_2) interactions using PBE-ZORA/TZ2P with dispersion correction. All values are in electron-volt, except for the Hirshfeld charges that are expressed in atomic units. Values between parenthesis are [a] the percentage contribution to ΔE^{int} and [b] the percentage contribution to ΔE^{orb}_{tot}. [c] q_1 and q_2 denote the Hirshfeld charges of each fragment, respectively.

	$Ir_4(CO)^{te}$	$Ir_4(CO)_4{}^{te}$	$Ir_4(O_2)^{te}$	$Ir_4(O_2)_4{}^{te}$	$Ir_4(PH_3)^{te}$	$Ir_4(PH_3)_4{}^{te}$	$Ir_4(SH_2)^{te}$	$Ir_4(SH_2)_4{}^{te}$
ΔE^{int}	−2.71	−3.31	−4.56	−5.23	−2.61	−2.75	−1.80	−2.09
ΔE^{Pauli}	13.06	11.66	12.45	11.92	22.18	9.74	8.62	7.51
ΔE^{elst}	−8.98	−8.47	−6.32	−6.42	−14.89	−7.90	−6.19	−5.75
[a] (%)	(56.90)	(56.58)	(37.13)	(37.42)	(60.06)	(63.19)	(59.36)	(59.84)
ΔE^{orb}_{tot}	−6.72	−6.41	−10.63	−10.67	−9.71	−4.43	−4.13	−3.73
[a] (%)	(42.57)	(42.79)	(62.49)	(62.19)	(39.18)	(35.48)	(39.64)	(38.84)
ΔE^{disp}	−0.08	−0.09	−0.06	−0.07	−0.19	−0.17	−0.10	−0.13
[a] (%)	(0.53)	(0.63)	(0.37)	(0.39)	(0.76)	(1.33)	(1.00)	(1.32)
ΔE^{orb}_1	−1.78	−1.75	−7.34	−6.20	−4.96	−1.47	−1.02	−1.11
[b] (%)	(26.46)	(27.30)	(69.04)	(58.15)	(51.04)	(33.17)	(24.58)	(29.86)
[b]ΔE^{orb}_2	−1.58	−1.60	−0.50	−1.41	−1.36	−0.78	−0.88	−0.75
[b] (%)	(23.53)	(25.00)	(4.69)	(13.19)	(14.03)	(17.57)	(21.27)	(19.99)
ΔE^{orb}_3	−1.63	−1.56	−0.73	−0.87	−1.01	−0.74	−0.70	−0.51
[b] (%)	(24.28)	(24.30)	(6.86)	(8.19)	(10.40)	(16.62)	(17.01)	(13.65)
ΔE^{orb}_{res}	−1.73	−0.70	−1.14	−1.27	−2.38	−0.64	−1.54	−0.59
[b] (%)	(25.73)	(23.40)	(19.41)	(20.47)	(24.53)	(32.64)	(37.14)	(36.50)
[c]q_1	0.2291	0.2465	0.3339	0.3612	−0.0483	0.0547	0.0102	0.0353
[c]q_2	−0.2290	−0.2477	−0.3334	−0.3614	0.0474	−0.0543	−0.0093	−0.0338

I Vibrational Frequencies

Bellow, we provided the vibrational frequencies ($3N-6$) of the lowest energy structures for bare and protected Ir_4 DFT-PBE+vdW+SOC nanoclusters, for Ir_4, $Ir_4(CO)_{12}$, $Ir_4(CO)_4$, $Ir_4(O_2)_4$, $Ir_4(PH_3)_4$, and $Ir_4(SH_2)_4$, for square and tetrahedral isomers. The vibrational frequencies were calculated employing the approach in which the Hessian matrix is calculated using finite differences as implemented in VASP. We employ two atomic displacements, i.e., each atom is displaced in each direction by ±0.010 Å. All the $3N-6$ (N is the number of atoms) vibrational frequencies are given in cm^{-1}.

Ir_4 - square

252.49 228.06 226.65 206.81 138.28 126.47

Ir_4 - tetrahedron

267.11 202.54 201.91 178.21 146.66 127.22

$Ir_4(CO)_{12}$ - rhombus

2100.68 2055.43 2052.23 2036.34 2033.74 2028.56

2012.93 2007.77 1999.50 1985.06 1880.79 1863.44

605.07 579.25 563.92 544.74 543.43 541.35

535.13 528.93 517.19 512.87 511.25 502.59

498.96 491.79 489.75 487.34 484.73 477.18

471.71 460.13 447.75 436.70 434.82 426.31

423.56 416.86 410.84 406.39 393.83 384.31

381.86 378.36 373.50 362.96 351.15 327.17

201.49 191.04 172.32 136.42 132.92 123.21

117.06 111.84 104.98 103.70 97.86 96.58

92.08 87.61 81.62 79.08 76.14 71.13

68.58 66.26 61.89 58.98 57.58 55.16

46.31 43.73 40.08 34.74 27.99 15.10

$Ir_4(CO)_{12}$ - tetrahedron

2093.54 2056.95 2056.19 2054.77 2022.84 2022.05

2021.34 2006.07 2005.08 1992.93 1990.86 1990.75

542.50 533.71 532.12 528.61 510.25 506.97

503.28 495.90 495.63 492.23 489.06 486.08

480.77 478.49 475.36 470.58 466.39 465.71

460.61 452.82 452.20 441.00 437.94 434.54

432.29 430.69 426.52 420.99 417.65 410.60

406.33 400.38 393.85 386.86 383.00 375.59

196.53 156.49 153.88 150.09 128.62 126.81

124.01 119.87 117.40 112.47 106.86 103.49

102.80 100.46 96.51 90.45 87.21 80.19

79.35 72.72 72.15 65.65 62.17 58.76

54.12 46.91 42.73 41.12 27.60 5.57

$Ir_4(CO)_4$ - square

2026.53 1989.42 1986.60 1979.57 500.24 495.66

483.99 474.76 459.00 439.43 419.36 413.30

396.13 378.99 373.84 353.52 211.73 209.41

205.06 202.83 124.51 109.54 93.26 75.59

71.19 62.96 58.74 41.92 32.16 23.95

$Ir_4(CO)_4$ - tetrahedron

2005.05 1975.17 1968.43 1965.45 570.95 553.33

543.18 541.28 527.95 521.88 510.49 497.88

491.70 489.07 480.65 474.74 237.60 177.23

173.31 158.15 125.34 121.88 96.41 90.32

79.59 72.98 66.88 58.37 46.38 39.99

$Ir_4(O_2)_4$ - square

1019.48 996.67 985.06 978.66 501.94 484.72

484.12 464.93 459.28 440.42 425.48 412.61

257.89 247.43 240.74 237.85 235.62 222.90

190.11 129.75 123.99 113.43 110.30 107.93

98.61 86.23 71.25 61.28 43.45 31.11

$Ir_4(O_2)_4$ - tetrahedron

984.78 979.03 969.62 962.82 540.48 531.97

527.47 497.28 478.65 468.68 459.30 452.74

247.94 236.52 216.19 208.35 206.96 184.58

172.61 166.68 159.07 134.02 118.81 109.25

101.24 95.70 90.15 78.97 78.39 58.14

$Ir_4(PH_3)_4$ - square

2375.40 2374.89 2370.72 2368.01 2337.25 2332.20

2329.20 2327.53 2306.88 2301.66 2301.02 2298.45

1117.17 1114.88 1113.40 1111.27 1058.11 1055.62

1054.07 1050.53 1018.99 1001.30 1000.43 995.48

536.07 534.32 530.34 512.96 483.43 481.24

479.00 478.09 357.03 350.77 341.43 341.03

215.56 214.47 214.23 211.61 161.98 154.82

150.17 145.09 104.60 86.97 74.63 72.24

55.33 51.45 48.23 28.82 13.46 8.10

$Ir_4(PH_3)_4$ - tetrahedron

2346.73 2345.62 2339.91 2338.50 2294.56 2289.93

2289.31 2288.29 2275.63 2273.07 2271.67 2271.11

1099.38 1096.45 1095.69 1094.99 1088.01 1083.94

1082.88 1080.42 1052.88 1039.74 1037.63 1034.57

588.09 584.50 582.35 578.11 564.68 558.50

557.97 552.76 395.00 388.03 385.83 384.01

233.82 187.93 160.42 158.48 143.78 138.15

135.37 133.54 124.98 123.20 109.26 103.08

96.40 87.60 81.41 75.87 70.41 66.83

$Ir_4(SH_2)_4$ - square

2480.22 2471.53 2469.07 2468.45 2440.33 2424.58

2421.34 2418.56 1207.86 1206.25 1200.40 1198.30

630.29 625.96 607.15 588.44 500.88 488.04

481.28 477.08 326.39 313.89 312.05 301.90

287.82 276.56 265.63 227.06 222.56 220.39

215.90 194.74 116.97 116.79 80.66 72.41

64.60 63.81 60.22 52.18 32.99 30.74

$Ir_4(SH_2)_4$ - tetrahedron

2409.34 2391.28 2385.13 2372.99 2369.72 2348.52

2342.30 2341.24 1175.53 1174.03 1171.58 1167.71

685.13 665.51 660.12 645.45 634.77 610.88

607.87 579.84 343.79 341.50 339.15 326.91

239.62 210.87 193.91 191.80 180.85 179.39

171.54 165.13 134.41 132.98 99.66 84.84

73.46 68.72 68.11 60.17 55.80 49.92

J Local Density of States

Bellow, in Figure 5 we show the local density of states (LDOS) for (a) Ir_4 square, (b) Ir_4 tetrahedron, (c) $Ir_4(CO)_{12}$ square, (d) $Ir_4(CO)_{12}$ tetrahedron, (e) $Ir_4(CO)_4$ square, (f) $Ir_4(CO)_4$ tetrahedron, (g) $Ir_4(O_2)_4$ square, (h) $Ir_4(O_2)_4$ tetrahedron, (i) $Ir_4(PH_3)_4$ square, (j) $Ir_4(PH_3)_4$ tetrahedron, (k) $Ir_4(SH_2)_4$ square, and (l) $Ir_4(SH_2)_4$ tetrahedron, where we show the LDOS for $Ir_4(Mol)_n$ (where Mol is equal to CO, O_2, PH_3, and SH_2, and n = 4 and 12), Ir_4, and $(Mol)_n$.

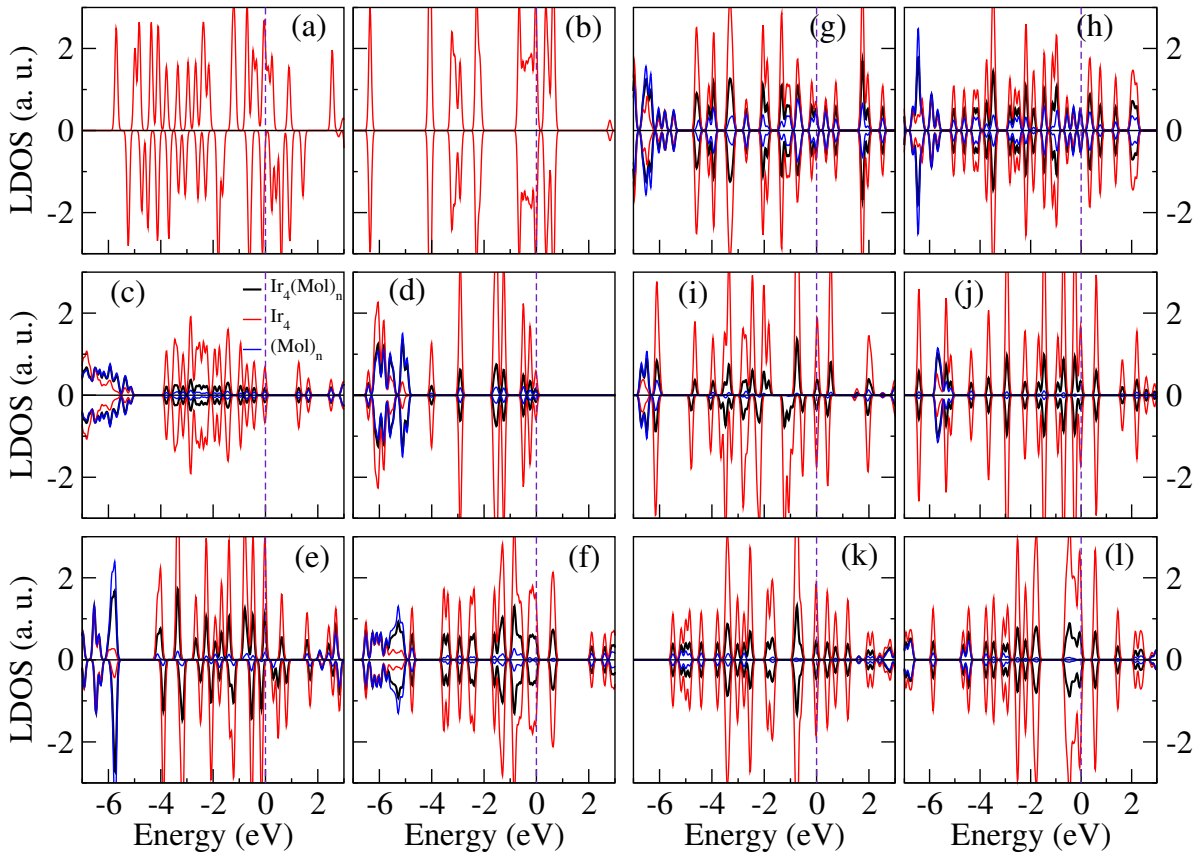

Figure 5: The local density of states (LDOS) of (a) Ir_4 square, (b) Ir_4 tetrahedron, (c) $Ir_4(CO)_{12}$ square, (d) $Ir_4(CO)_{12}$ tetrahedron, (e) $Ir_4(CO)_4$ square, (f) $Ir_4(CO)_4$ tetrahedron, (g) $Ir_4(O_2)_4$ square, (h) $Ir_4(O_2)_4$ tetrahedron, (i) $Ir_4(PH_3)_4$ square, (j) $Ir_4(PH_3)_4$ tetrahedron, (k) $Ir_4(SH_2)_4$ square, and (l) $Ir_4(SH_2)_4$ tetrahedron. The LDOS is shown for $Ir_4(Mol)_n$ (where Mol is equal to CO, O_2, PH_3, and SH_2, and n = 4 and 12), for Ir_4, and for $(Mol)_n$. The Fermi level is at zero energy and a Gaussian broadening with a width of 0.1 eV has been applied.

K Atomic Positions

Bellow, we provided the atomic positions (xyz coordinates) for Ir_4 DFT-PBE isomers, as showed in the main article and according to the Table 5.

Ir_4 configuration (a) - square

Ir 0.6263304999999999 0.9388704999999993 -1.2063047500000001

Ir -1.2839344999999991 1.0305555000000011 0.1353912499999987

Ir 1.2836665000000007 -1.0308214999999992 -0.1357537499999983

Ir -0.6260625000000015 -0.9386045000000012 1.2066672499999997

Ir_4 configuration (b) - butterfly

Ir -0.2240259999999985 1.7586422499999985 -0.2065107499999996

Ir 0.9441869999999994 0.1171762500000009 1.0129242500000011

Ir 0.6185569999999991 -1.5598507499999981 -0.6078987500000004

Ir -1.3387180000000001 -0.3159677500000013 -0.1985147500000011

Ir_4 configuration (c) - rhombus

Ir -1.9290997499999980 0.6434824999999984 0.3481774999999994

Ir 0.4021222499999988 1.2079515000000010 -0.0048784999999993

Ir 1.9300002500000000 -0.6438134999999994 -0.3425324999999999

Ir -0.4030227500000008 -1.2076205000000000 -0.0007665000000001

Ir_4 configuration (d) - triangle-capped

Ir -1.5658842500000008 -1.2063632500000008 0.0564962499999995

Ir 0.1374067499999994 0.4518207500000013 -0.0074497499999984

Ir 0.7521397500000004 -1.8362382499999992 0.0538182500000000

Ir 0.6763377500000010 2.5907807499999986 -0.1028647500000011

Ir_4 configuration (e) - tetrahedron

Ir -0.8630162499999976 0.5894394999999992 1.0801895000000004

Ir 0.7434457499999994 1.1005485000000004 -0.7035974999999999

Ir -0.8642392500000007 -0.7322034999999989 -0.9879755000000001

Ir 0.9838097499999989 -0.9577845000000007 0.6113834999999996

Ir_4 configuration (f) - zigzag

Ir -0.9740697500000008 0.5044377500000001 0.2317982500000015

Ir 0.9846532500000018 -0.5301272500000005 -0.2428037499999993

Ir 3.0441442499999996 0.2205427499999990 0.1902502499999992

Ir -3.0547277500000005 -0.1948532499999986 -0.1792447500000014

Ir_4 configuration (g) - line

Ir -1.0931910000000009 0.0599295000000009 -0.0007687499999989

Ir 1.0932640000000013 -0.0597915000000011 0.0007932500000010

Ir 3.3219870000000000 -0.1744915000000002 -0.0011097500000012

Ir -3.3220600000000005 0.1743535000000005 0.0010852499999991

Bellow, we provided the atomic positions (xyz coordinates) for bare and protected Ir_4 DFT-PBE+vdW+SOC nanoclusters, as showed in Figure 2 of the article.

Ir_4 (*i*) - square

Ir 0.8453727499999992 1.0790924999999998 -0.8970654999999983

Ir -1.0500722499999995 1.1634064999999989 0.4749014999999996

Ir 1.0500827500000014 -1.1634854999999984 -0.4748855000000010

Ir -0.8453832500000011 -1.0790135000000003 0.8970494999999996

Ir_4 (*i*) - tetrahedron

Ir -0.8747035000000007 0.5708689999999992 1.0889632499999999

Ir 0.7564355000000003 1.0825229999999992 -0.7275917500000011

Ir -0.8814694999999997 -0.7168689999999982 -0.9927767500000000

Ir 0.9997375000000002 -0.9365230000000002 0.6314052500000011

$Ir_4(CO)_{12}$ (*ii*) - rhombus

Ir 1.3830108571428590 0.7481085714285719 -1.7584337499999989

Ir -0.9062141428571429 1.1732255714285720 -0.1318757499999996

Ir 1.0039988571428560 -0.9600064285714275 0.1865832500000011

Ir -1.4745581428571426 -1.0812564285714275 1.6591282500000013

C -2.2375591428571417 -2.2050084285714271 0.3080772499999995

C -1.8224551428571423 0.1201255714285715 -1.4769417499999988

C 1.1440558571428583 0.7516315714285696 -3.6427737500000008

C 2.1525588571428558 -1.1845694285714274 -1.4988117499999987

C -2.9636521428571441 -1.3301614285714281 2.7512952500000010

C -0.4029601428571446 -0.5224184285714294 3.1428152500000008

C 0.7125258571428561 -2.8023584285714294 0.5627962500000010

C 2.2803738571428576 -0.7842874285714302 1.5270062499999988

C 0.1008848571428573 2.4126385714285710 -1.5039327500000013

C 3.0058838571428574 1.7161035714285706 -1.7788997500000014

C -2.4510331428571432 2.1775005714285718 0.3082662499999984

C 0.1321708571428588 1.8735055714285718 1.3432222499999995

O -2.6594471428571445 -2.9845654285714276 -0.4411577499999992

O 2.8734798571428564 -1.9621534285714284 -2.0221417500000003

O 1.0183538571428579 0.6935235714285725 -4.7942097500000003

O -2.3784051428571416 -0.4410454285714301 -2.3238097499999997

O 0.6670318571428582 -3.9528074285714276 0.7162592499999996

O 0.2489558571428589 -0.3030084285714295 4.0781462499999996

O 3.1316158571428567 -0.6385264285714299 2.3070152499999983

O -0.0097111428571438 3.5138425714285706 -1.9143497500000002

O 4.0177908571428578 2.2829765714285712 -1.8119637500000010

O 0.7402628571428580 2.3581315714285700 2.2011202499999980

O -3.4021511428571443 2.7808155714285703 0.5832042500000008

O -3.9048081428571435 -1.4499564285714279 3.4243662499999976

$Ir_4(CO)_{12}$ (*ii*) - tetrahedron

Ir -0.9502181785714294 0.6617848214285701 1.2157787142857159

Ir 0.8323668214285715 1.2279008214285709 -0.7856592857142843

Ir -0.9776321785714297 -0.8027391785714272 -1.0984222857142847

Ir 1.0968268214285712 -1.0766251785714283 0.6675477142857147

C 0.3871748214285728 -2.6017351785714298 1.5682627142857128

C -0.1755801785714299 2.6542638214285730 -1.5560622857142861

C -2.2608221785714271 0.2276698214285716 -2.0636852857142847

C -1.9499451785714295 -0.5413791785714274 2.3094017142857135

C -0.0849051785714290 1.6967038214285726 2.5665787142857157

C -2.3373181785714294 1.8655558214285701 0.6948037142857160

C 2.2933698214285734 -0.4285021785714299 2.0062087142857132

C 2.3463348214285702 -1.9219271785714285 -0.5030142857142856

C -2.0907971785714281 -2.2009471785714276 -0.4286662857142852

C -0.1367831785714275 -1.7111771785714276 -2.5501702857142865

C 2.0955528214285728 2.2299458214285699 0.2346427142857130

C 1.9141678214285702 0.7411858214285708 -2.2806862857142844

O -3.0328231785714266 0.8505148214285697 -2.6651912857142852

O -2.5495291785714294 -1.2720091785714289 2.9821807142857155

O -0.7802331785714289 3.5353178214285723 -2.0079242857142843

O -0.0431381785714289 -3.5347141785714293 2.1071897142857141

O 3.0168368214285728 -0.0500531785714301 2.8304227142857146

O 3.1176778214285719 -2.4301211785714281 -1.2050392857142846

O 0.4333218214285706 2.3367398214285706 3.3839007142857165

O -3.1919231785714288 2.5843878214285723 0.3806047142857138

O 2.8802018214285710 2.8263158214285702 0.8468657142857132

O 2.5605528214285727 0.4529738214285729 -3.1998492857142855

O 0.3681928214285717 -2.2785731785714298 -3.4270072857142848

O -2.7809291785714265 -3.0407571785714276 -0.0230112857142857

$Ir_4(CO)$ (*iii*) - square

Ir -0.3908859999999990 0.4760020000000011 -1.9244563333333335

Ir 0.3747390000000010 0.2164760000000001 0.3039396666666665

Ir 0.2365150000000000 -1.6608769999999993 -2.4258463333333342

Ir 1.0150999999999999 -1.9791130000000017 -0.2628313333333328

C -0.3473550000000010 1.2185020000000009 1.7021826666666673

O -0.8881130000000013 1.7290099999999988 2.6070116666666667

$Ir_4(CO)$ (*iii*) - tetrahedron

Ir -1.5528791666666664 1.3186261666666650 0.6594073333333346

Ir -0.5971831666666667 2.0884111666666674 -1.3822706666666662

Ir -1.3792971666666667 -0.2168578333333318 -1.2349426666666681

Ir 0.7744028333333339 0.2772881666666653 -0.1412066666666684

C 1.2631318333333332 -1.2327688333333344 0.7636493333333338

O 1.4918248333333330 -2.2346988333333324 1.3353633333333341

$Ir_4(O_2)$ (*iv*) - square

Ir -0.3995153333333341 0.7543643333333320 -1.8346386666666668

Ir -0.0053843333333325 0.2379843333333339 0.4328373333333317

Ir 0.0583626666666668 -1.4164406666666660 -2.4201086666666676

Ir 0.4519626666666661 -1.9629246666666655 -0.1929206666666659

O -0.4146983333333345 1.7204283333333317 1.6886943333333342

O 0.3092726666666679 0.6665883333333339 2.3261363333333342

$Ir_4(O_2)$ (*iv*) - tetrahedron

Ir -0.2111735000000003 0.2176628333333337 0.3352505000000008

Ir 1.1359254999999997 0.7567848333333327 -1.5934644999999996

Ir -0.2587564999999998 -1.2344471666666674 -1.7987745000000004

Ir 1.6920934999999993 -1.3285841666666673 -0.4425545000000000

O -1.7671544999999995 0.8390868333333348 1.3369534999999999

O -0.5909344999999988 0.7494968333333336 2.1625894999999993

$Ir_4(PH_3)$ (*v*) - square

Ir 1.5953242500000009 2.3315582500000009 -2.6003278750000005

Ir -0.2831537500000003 2.2598462499999994 -1.2686768749999997

Ir 2.2386842499999986 0.2477532499999994 -1.8432458750000000

Ir 0.3301832500000010 0.1564522500000015 -0.4710878750000012

P -0.7539937499999994 -0.9669837500000001 1.1612891250000006

H -0.1069487500000008 -2.1549487499999986 1.6003381250000013

H -2.0607927500000010 -1.5079227500000019 0.9863401249999990

H -0.9593027499999991 -0.3657547500000001 2.4353711250000005

$Ir_4(PH_3)$ (*v*) - tetrahedron

Ir -0.9389606250000000 1.9708977499999982 1.2439142500000004

Ir 0.6624583749999999 2.6522517500000005 -0.5046407499999992

Ir -0.9772776249999993 0.8777767499999982 -0.9724997499999999

Ir 1.1516863750000006 0.6965517500000005 0.9020632499999985

P 0.0774003749999999 -0.9578742500000004 -0.1873087499999988

H 0.8397103749999992 -1.7336832499999992 -1.1143547499999995

H -1.1738816249999999 -1.7071552500000002 -0.3565557500000009

H 0.3588643749999996 -1.7987652499999995 0.9893822499999994

$Ir_4(SH_2)$ (*vi*) - square

Ir 1.4737535714285703 2.1570282857142864 -2.2821495714285729

Ir -0.3803244285714275 2.3980542857142844 -0.8928105714285698

Ir 1.7999765714285727 0.0256502857142848 -1.4983765714285728

Ir -0.0616674285714293 0.2398322857142858 -0.0842165714285704

S -1.1107534285714282 -1.0174747142857150 1.4442464285714283

H -0.2496734285714272 -1.5610577142857132 2.3547974285714299

H -1.4713114285714293 -2.2420327142857133 0.9585094285714278

$Ir_4(SH_2)$ (*vi*) - tetrahedron

Ir -2.2218015714285713 1.8946689999999997 0.1176904285714291

Ir -0.3925685714285727 2.2857170000000009 -1.3847565714285710

Ir -1.6864505714285727 0.2504500000000001 -1.6212885714285714

Ir -0.4535655714285696 0.1702919999999992 0.4614044285714277

S 1.2602064285714292 -1.0640030000000003 1.0875024285714301

H 2.3439814285714284 -1.1073570000000010 0.2573564285714274

H 1.1501984285714286 -2.4297680000000001 1.0820914285714278

$Ir_4(CO)_4$ (*vii*) - square

Ir 0.6669912500000001 0.5690824999999990 -1.5076494166666674

Ir -1.3962877500000010 0.9708135000000007 -0.3804494166666654

Ir 0.9654202499999989 -1.4301934999999990 -0.2502334166666682

Ir -1.1007097499999985 -1.0330984999999988 0.8687545833333334

C -2.0178917499999991 -1.4341644999999990 2.4672635833333336

C -2.2588547499999998 2.6483395000000010 -0.3280494166666667

C 2.0483082499999994 1.4711474999999996 -2.4216794166666675

C 2.2933942500000000 -2.6160855000000018 0.3783615833333325

O -2.5270437499999994 -1.6390804999999997 3.4945885833333348

O 3.1388922499999992 -3.2825795000000020 0.8222935833333327

O 2.9206032500000005 2.0678894999999984 -2.9109594166666648

O -2.7328217500000016 3.7079295000000005 -0.2322414166666650

$Ir_4(CO)_4$ (*vii*) - tetrahedron

Ir -1.3307008333333346 0.4271836666666660 1.5299468333333324

Ir 0.3503941666666646 0.9952216666666671 -0.2756721666666678

Ir -1.2002418333333327 -0.9263973333333325 -0.6694231666666660

Ir 0.6926941666666662 -1.0733163333333329 1.0871818333333345

C 2.0165661666666672 -2.0205613333333319 0.2257608333333344

C 1.5252161666666668 0.9325366666666652 -1.7141141666666662

C -2.5485988333333331 -0.2401273333333321 -1.7031601666666680

C -0.7970988333333326 1.3901076666666670 2.9841818333333330

O -3.3984008333333335 0.2764076666666655 -2.3221941666666672

O -0.3785358333333337 2.0059526666666669 3.8919898333333323

O 2.2446201666666674 0.8195746666666657 -2.6279891666666670

O 2.8240861666666675 -2.5865823333333346 -0.4065081666666664

$Ir_4(O_2)_4$ (*viii*) - square

Ir 1.1454700000000004 0.5754302499999990 -1.0299916666666680

Ir 0.7001350000000004 -1.4856567500000013 -0.0666336666666648

Ir -0.7178110000000002 1.4805642499999996 0.0400283333333352

Ir -1.1277150000000011 -0.5655767499999993 1.0498513333333324

O -2.8987860000000003 -1.1904657499999987 1.7014833333333321

O -1.7236549999999999 3.0918442499999998 -0.5388496666666679

O -1.9485920000000005 -1.2766227499999987 2.7128883333333356

O -1.2805209999999994 3.2374612500000013 0.7727763333333325

O 2.7048980000000009 1.5971582499999990 -1.7196816666666668

O 0.9759740000000017 -3.4110297499999986 -0.4585636666666669

O 2.0466109999999995 -2.8989657499999999 0.2731013333333326

O 2.1239919999999985 0.8458592499999991 -2.7364086666666658

$Ir_4(O_2)_4$ (*viii*) - tetrahedron

Ir -1.0001392500000006 0.8069187500000012 0.9152864999999984

Ir 0.8466437500000016 1.2324217500000003 -0.5052554999999991

Ir -0.9948672499999990 -0.8934122500000008 -0.7217065000000019

Ir 1.1273347499999988 -0.9511802500000002 0.3468755000000009

O 1.7472057499999991 -2.3094072499999996 1.6404145000000003

O 2.6711007500000008 -2.1021862499999990 0.5912054999999988

O 1.4562897499999994 2.2553937499999996 -2.0247274999999996

O 2.0419107499999996 2.7790407500000001 -0.8551695000000009

O -2.3895932500000008 1.9099877499999991 1.8082295000000013

O -1.6950432499999981 1.0674337499999993 2.6977574999999994

O -1.4494112500000012 -1.7234772499999984 -2.4565964999999985

O -2.3614312499999990 -2.0715332500000017 -1.4363134999999994

$Ir_4(PH_3)_4$ (*ix*) - square

Ir 0.9010520499999999 0.7858010499999993 -1.1555959999999990

Ir -1.1296099499999996 1.2134670500000015 -0.0177359999999991

Ir 1.1640720500000008 -1.2273329500000014 0.0628260000000013

Ir -0.8723869500000000 -0.7984389499999983 1.2032169999999989

P -1.4023629500000012 -2.2772179500000016 2.8089750000000002

P -3.0195849499999996 2.3689060499999988 0.3595499999999989

P 1.3829900499999994 2.2821030499999990 -2.7607460000000010

P 3.0426240499999997 -2.3741069499999989 -0.3972030000000009

H -1.6719089499999995 -3.6582299500000000 2.5608620000000002

H -2.6150149499999999 -1.9696349500000001 3.4869689999999984

H -0.5826109500000002 -2.4683129499999987 3.9619980000000012

H 3.1167980499999990 -3.6374239499999996 0.2526359999999991

H 3.3859180499999999 -2.8158949500000015 -1.7109090000000007

H 4.3388860499999984 -1.8966689499999991 -0.0351919999999984

H 2.5994030499999985 2.0188370500000010 -3.4498330000000017

H 1.6067280500000003 3.6699660499999984 -2.5058819999999997

H 0.5455680499999993 2.4508860500000003 -3.9043059999999983

H -3.1228179499999991 3.5361140500000010 -0.4471130000000015

H -4.3078409500000001 1.8226050499999991 0.0789299999999999

H -3.3599009500000010 2.9745770499999997 1.6085530000000008

$Ir_4(PH_3)_4$ (*ix*) - tetrahedron

Ir -0.0490242000000009 0.9684816999999999 1.2146751499999997

Ir 1.1648348000000019 0.3565987000000010 -0.9640078499999998

Ir -1.3073982000000008 0.0923236999999997 -0.8413038500000010

Ir 0.1823848000000020 -1.4235872999999994 0.5933791499999987

P 1.8091487999999998 -2.1749182999999999 1.8581061499999993

P 1.4725797999999990 2.2068947000000012 -2.0976538499999986

P -1.8294121999999995 -1.0211522999999989 -2.6560788499999983

P -1.4543402000000001 0.9875837000000001 2.8962561500000010

H -0.9921871999999994 -2.1027523000000006 -3.0552678500000017

H -3.0732302000000007 -1.7220282999999998 -2.7821818499999988

H -1.8956702000000007 -0.3894263000000020 -3.9410198500000018

H -2.1729282000000008 2.1713906999999981 3.2652921499999987

H -1.0449271999999994 0.6519187000000013 4.2283281500000012

H -2.5806251999999996 0.1171176999999997 2.8517831500000010

H 1.3224068000000002 2.2565277000000012 -3.5216798499999999

H 2.7186758000000002 2.9144677000000012 -2.0639428499999983

H 0.6414738000000006 3.3280666999999990 -1.8110508499999991

H 2.8990878000000007 -1.3035613000000001 2.1435901499999996

H 2.5986388000000002 -3.3077503000000004 1.4750661499999982

H 1.5905117999999987 -2.6061953000000013 3.2077111499999997

$Ir_4(SH_2)_4$ (*x*) - square

Ir 0.6254472499999983 0.9963357499999992 -1.1472595625000015

Ir -1.2405157499999988 0.8583507499999987 0.2825294375000016

Ir 1.4422332499999988 -1.0208032500000011 -0.2746935624999989

Ir -0.4173037500000008 -1.1624832499999984 1.1517574375000013

S -1.4149197500000015 -2.4132562500000008 2.7315034375000016

S -2.9315747500000011 2.3301177499999985 0.4130774374999990

S 1.8351342500000010 2.0206257499999998 -2.7664595625000006

S 3.1195082500000009 -2.5097182499999997 -0.4042085625000003

H -2.7253137499999998 -2.6904642499999989 2.4575744374999990

H -1.7569127500000001 -1.7202642500000005 3.8598664375000009

H 2.7118832500000014 -3.8035872500000005 -0.5757815624999989

H 3.7032942500000008 -2.8112132499999989 0.7953104374999984

H 1.0545172500000013 2.3333867500000016 -3.8430355624999999

H 2.0346962500000014 3.3400247500000004 -2.4750225624999986

H -2.5329687500000002 3.6267107500000000 0.5864454374999990

H -3.5072047500000014 2.6262377500000005 -0.7916035624999982

$Ir_4(SH_2)_4$ (*x*) - tetrahedron

Ir -1.1818733125000005 0.6179360625000007 0.8939545000000009

Ir 0.5056666875000015 1.1702590624999982 -0.9123505000000010

Ir -1.1771393125000014 -0.6901899375000008 -1.2494405000000008

Ir 0.6921006875000000 -0.9304279374999987 0.3943774999999987

S 2.4250506874999989 -1.0222019374999998 1.8198495000000017

S 1.8470886874999994 1.3001340625000002 -2.6822154999999999

S -2.6392853124999984 -2.3557389374999995 -1.0942205000000009

S -0.8745663124999989 1.8931340625000002 2.7019225000000002

H -2.4570693125000016 -3.2715749375000018 -2.1088955000000009

H -3.8391763124999994 -1.9921689375000002 -1.6654575000000009

H -1.7224133125000005 1.5407060625000004 3.7304125000000017

H -1.5619003124999988 3.0761040625000011 2.5583985000000009

H 2.8381236874999995 2.2491260625000007 -2.5331925000000002

H 1.2517496875000003 2.0922520624999987 -3.6357245000000002

H 3.5279126875000006 -1.5302649374999997 1.1743195000000006

H 2.3657306874999993 -2.1470839374999993 2.6082625000000004